

Enhanced Structural and Morphological Properties of Doped Cobalt Zinc Ferrite

Asmaa Reda Abd El-Salam^{1*}, K. E. Rady^{2,3}, Ezzat A. ELFadaly¹, Mobarak Hassan Aly¹

¹Environmental Studies and Research Institute, University of Sadat City, Sadat City, Menoufia, Egypt

²Engineering Basic Science Department, Faculty of Engineering, Menoufia University

³Basic Sciences Department, Higher Institute of Engineering and Technology, MNF-HIET, Menoufia, Egypt

*Correspondence should be addressed to Asmaa Reda Abd El-Salam, Asmaa.reda@esri.usc.edu.eg, asmaa_reda@yahoo.com

Received date: October 11, 2023, **Accepted date:** October 19, 2023

Citation: El-Salam AR, Rady KE, ELFadaly EA, Aly MH. Enhanced Structural and Morphological Properties of Doped Cobalt Zinc Ferrite. J Nanotechnol Nanomaterials. 2023;4(2):89-93.

Copyright: © 2023 El-Salam AR, et al. This is an open-access article distributed under the terms of the Creative Commons Attribution License, which permits unrestricted use, distribution, and reproduction in any medium, provided the original author and source are credited.

Abstract

In this study, Mn²⁺ substituted Co_{0.8-x}Mn_xZn_{0.2} (where x = 0.0, 0.1, 0.2, and 0.3) ferrites are prepared by a coprecipitation method to study the effect of Mn²⁺ ions on the structural and morphological properties. These ferrites are characterized by X-ray powder diffraction (XRD), and Fourier transform infrared. X-ray diffraction patterns of the prepared samples confirm partial substitution of Mn²⁺ ions that does not change the basic structure of Co_{0.8}Zn_{0.2}Fe₂O₄. It also provides information about the formation of a single-phase spinel structure without any secondary phase. It is concluded that Co_{0.6}Mn_{0.2}Zn_{0.2}Fe₂O₄ has a spherical shape with an average particle size of 22.51 nm based on TEM, as confirmed by the XRD analysis. FT-IR analysis confirms the formation of vibrational frequency bands associated with the entire spinel structure. The IR spectra of ferrites show two clear and sharp absorption bands in the range of 442.09 and 620.21 cm⁻¹ in the range of 200–1000 cm⁻¹, which confirms the formation of the ferrite composite.

Keywords: AC conductivity, Co-precipitation method, Co–Zn ferrites, FTIR, Mn²⁺ substituted Co–Zn ferrite, XRD

Introduction

Several years of worldwide revolutionary developments in nanoscience, combining physics, chemistry, material science, theory, and even biosciences, have brought us to another level of understanding. The remarkable progress in science and technology is established with the advancement in nanoscience and nanotechnology. Nanoscience and nanotechnology represent an expanding research area, which involves structures, devices, and systems with novel properties and functions due to the arrangement of their atoms on the 1–100 nm scale [1]. Basically, ferrites are ceramic materials, dark grey or black in appearance and very hard and brittle. Ferrites may be defined as magnetic materials composed of oxides containing ferric ions as the main constituent (the word ferrite comes from the Latin “ferrum” for iron) and classified as magnetic materials because they exhibit ferrimagnetic behavior [2]. The ferrites, in powder or thin film forms, can be prepared by high-temperature solid-state reaction method, sol–gel method, coprecipitation, pulsed laser deposition,

high-energy ball milling and hydrothermal technique [3]. Ferrites have much less electrical conductivity compared to metallic ferro magnets, continues to be the most important magnetic materials in various high-frequency applications, having repressed eddy currents and lowered energy loss in high-frequency use. The ferrites are ionic in nature and are more stable because of their oxide bonding which exists between the metal ions. Therefore, ferrites are playing a great role in many devices of every-day life (ac and dc motors, power distribution systems, video and audio applications, microwave devices, antenna rods, loading coils, core material for power transformers in electronics, high-frequency devices [4-6], memory devices such as hard disks, floppy disks [6-8], capacitor electrode, catalysis [5,8], drug delivery [5], water treatment [9], and gas sensors [5].

This study demonstrates the expansion of lattice constant (*a*) and crystallite size (*D*) induced by manganese substituted of cobalt zinc ferrites exerted remarkable effects on its structural and morphological properties that suggested the material

with composition $\text{Co}_{0.8-x}\text{Mn}_x\text{Zn}_{0.2}\text{Fe}_2\text{O}_4$ may be suitable for high frequency application and in transformer cores.

The aim of this research work is to investigate the effect of Mn^{2+} on the structural and morphological properties of new $\text{Co}_{0.8-x}\text{Mn}_x\text{Zn}_{0.2}\text{Fe}_2\text{O}_4$ ferrite materials synthesized by coprecipitation method.

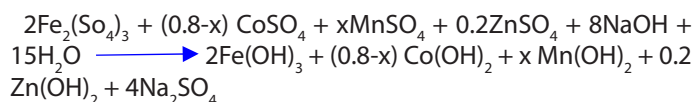
Methods

Sample preparation

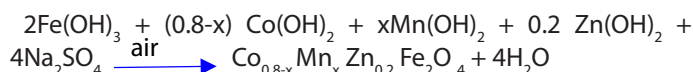
$\text{Co}_{0.8-x}\text{Mn}_x\text{Zn}_{0.2}\text{Fe}_2\text{O}_4$ ($x=0.0$ to 0.3 with a step 0.1) ferrite materials are synthesized in the form of powder by coprecipitation method. The powder preparation and pellet preparation are discussed in [10].

A series of $\text{Co}_{0.8-x}\text{Mn}_x\text{Zn}_{0.2}\text{Fe}_2\text{O}_4$ ($x = 0.0$ to 0.3 with a step size of 0.1) nano ferrites prepared using the coprecipitation method. In this method, dissolving $\text{Fe}_2\text{SO}_4 \cdot x\text{H}_2\text{O}$, $\text{CoSO}_4 \cdot 7\text{H}_2\text{O}$, ZnSO_4 and $\text{MnSO}_4 \cdot \text{H}_2\text{O}$ with purity above 97% into distilled water to form a clear solution and mixed together. The mixture was stirred with a magnetic stirrer until the reactant was dissolved completely. During the stirring, sodium hydroxide was added dropwise to the salt solution as a precipitating agent. As a result, a brown precipitate appeared quickly. The pH of the solution reached 12 under vigorous stirring. Simultaneously, the mixed solution was heated to 80°C to transform into a black solution and subsequently maintained for 45 min to obtain good results for the reaction process and then the sufficient precipitation phase was observed as reported in [10].

The following ferrite materials with typical formula are synthesized in this research work. The chemical reactions in this process and specific amounts of each composition in mole, are given in the following equations [10]:



Then, air is passed over the metal hydroxide to oxidize it and to produce $\text{Co}_{0.8-x}\text{Mn}_x\text{Zn}_{0.2}\text{Fe}_2\text{O}_4$.



Sample Characterization

Structural characterization was studied using an X-ray diffractometer (D8 ADVANCE) with $\text{Cu-K}\alpha$ ($\lambda = 1.5406 \text{ \AA}$) radiation. The crystal structure, lattice parameter, crystallite size, and theoretical density were calculated from the XRD pattern. The FTIR absorption spectra of the samples were recorded using the FTIR spectrometer in the wave number range of $1000\text{--}100 \text{ cm}^{-1}$ with potassium bromide (KBr) as the solvent. We conducted transmission electron microscopy (TEM) to analyze the sample's topography and morphological features of the nanoparticles. The AC conductivity (σ_{ac}), dielectric constant (ϵ'), and dielectric loss angle ($\tan \delta$) of the prepared samples were determined at room temperature (300 K) as a function of frequency ranging from 50 Hz to 5 MHz using an LCR Bridge (HIOKI) Model 3531 Z HI tester.

Results and Discussion

X-ray analysis

The structure of the synthesized $\text{Co}_{0.8-x}\text{Mn}_x\text{Zn}_{0.2}\text{Fe}_2\text{O}_4$ ($x=0$ to 0.3 with a step 0.1) powder ferrites are analyzed by powder XRD between the Bragg angles 20° and 80° . Indexing process of powder diffraction pattern is done and Miller indices ($h k l$) to each peak are assigned, as shown in **Figure 1**. All the peaks present in the XRD patterns are very sharp because of

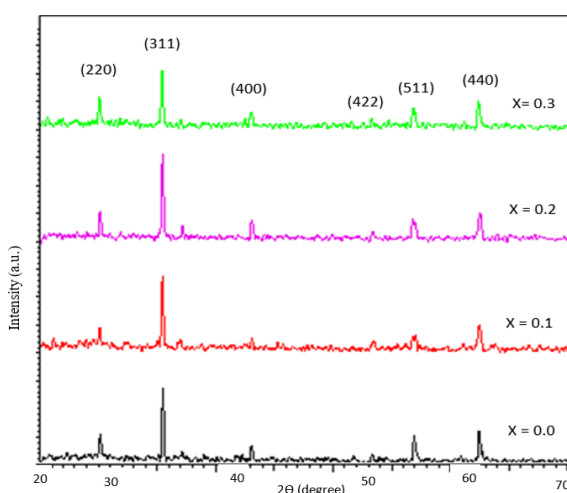


Figure 1. XRD pattern of $\text{Co}_{0.8-x}\text{Mn}_x\text{Zn}_{0.2}\text{Fe}_2\text{O}_4$ nanoparticle.

the micrometer size of the crystallite and they are indexed as (220), (311), (400), (422), (511), and (440) planes of spinel structure. The XRD patterns clearly indicate that $\text{Co}_{0.8-x}\text{Mn}_x\text{Zn}_{0.2}\text{Fe}_2\text{O}_4$ ferrites are formed in cubic single spinel phase without impurity. Further, the samples are identified as of single phase structure with a space group Fd3m, which is in well agreement with (JCPDC card no.22-1086) for CoFe_2O_4 [10-12].

The values of the lattice parameters were calculated using X-ray data using the following equation [13], and the results are shown in **Table 1**. The obtained results are shown in **Table 1**.

$$d_{hkl} = \frac{a}{\sqrt{h^2 + k^2 + l^2}} \quad (2)$$

| Table 1. Structural analysis of synthesized $\text{Co}_{0.8-x}\text{Mn}_x\text{Zn}_{0.2}\text{Fe}_2\text{O}_4$ Samples. | |
|-------------------------------------------------------------------------------------------------------------------------|----------------------|
| Content | a_{exp} (Å) |
| 0.0 | 8.3256 |
| 0.1 | 8.3777 |
| 0.2 | 8.391 |
| 0.3 | 8.377 |

As indicated in the table, the calculated lattice parameters, increased from 8.3256 to 8.377 Å with the Mn^{2+} concentration.

This occurred because the radius of Co^{2+} ions (0.78 Å) was smaller than that of the Mn^{2+} ions (0.80 Å) [14]. Thus, the substitution by larger ions resulted in the lattice expansion, leading to an increase in the lattice constant [15,16]. When the Co ions were replaced with manganese at $x = 0.3$, the lattice parameters decreased to 8.377 Å [17]. This decrease occurs because some Mn ions cannot enter lattice sites and stress on the grains. Consequently, the lattice constant decreased, and a similar behavior was observed [16].

Morphological analysis

TEM study is employed to investigate the morphological studies for the prepared sample of $\text{Co}_{0.6}\text{Mn}_{0.2}\text{Zn}_{0.2}\text{Fe}_2\text{O}_4$. **Figure 2** shows the TEM images of $\text{Co}_{0.6}\text{Mn}_{0.2}\text{Zn}_{0.2}\text{Fe}_2\text{O}_4$. TEM images demonstrated a spherical shape of the prepared sample, and the agglomerations observed may be related to the interactions of magnetic dipoles arising within the ferrite nanoparticle [13,18].

The morphological studies for the prepared sample of $\text{Co}_{0.6}\text{Mn}_{0.2}\text{Zn}_{0.2}\text{Fe}_2\text{O}_4$ were investigated through TEM analysis. **Figure 3** shows the TEM image of the prepared sample ($x = 0.2$). It can be seen from the TEM image that the sample is uniform in the morphology and particle size distribution. The average particle size was calculated via TEM analysis and was found to be 23.26 nm.

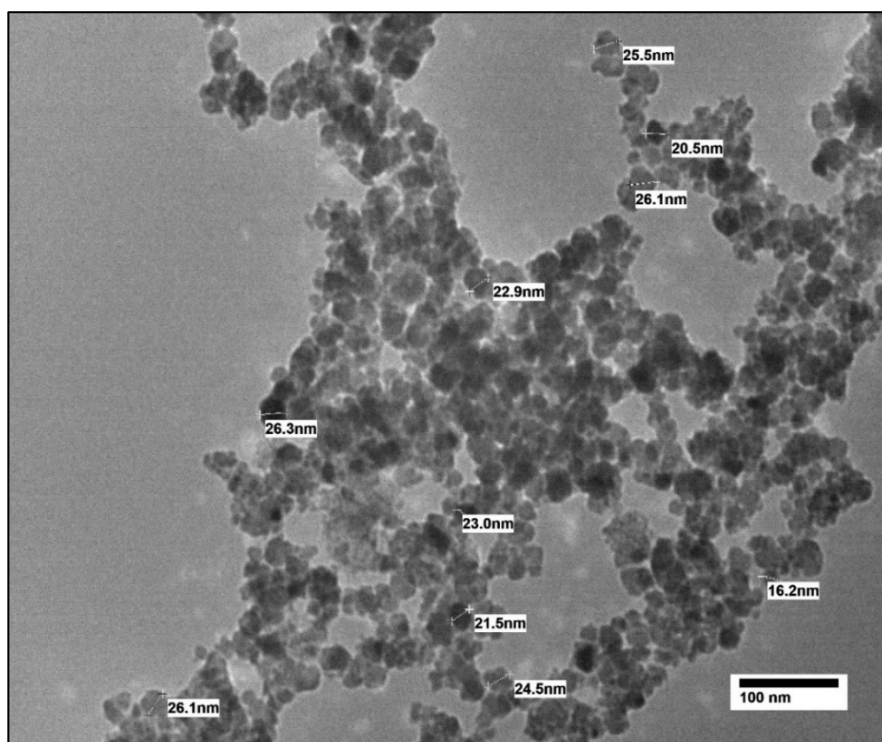


Figure 2. TEM image of $\text{Co}_{0.6}\text{Mn}_{0.2}\text{Zn}_{0.2}\text{Fe}_2\text{O}_4$ sample.

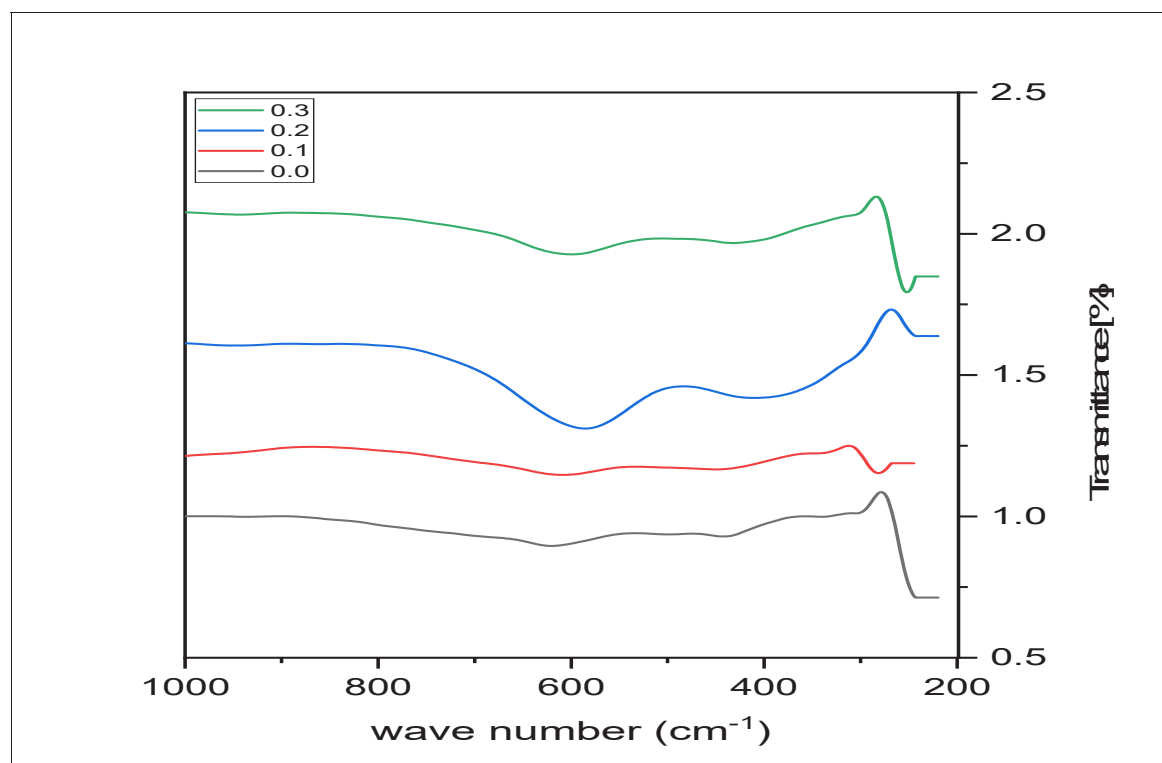


Figure 3. FTIR pattern of $\text{Co}_{0.8-x}\text{Mn}_x\text{Zn}_{0.2}\text{Fe}_2\text{O}_4$ nanoparticles.

Fourier transform infrared spectroscopy analysis

The FTIR spectroscopy of $\text{Co}_{0.8-x}\text{Mn}_x\text{Zn}_{0.2}\text{Fe}_2\text{O}_4$ ($x = 0.0$ to 0.3 with a step size of 0.1) was recorded in the range of $200\text{--}1000\text{ cm}^{-1}$. **Figure 3** shows the FTIR spectra of the prepared samples, and the absorption band results are presented in **Table 2**. It shows two absorption bands, ν_1 and ν_2 , at ~ 600 and 400 cm^{-1} , respectively, confirming the formation of the spinel structure. The high-frequency band (ν_1) corresponds to bending vibrations at the A site, and the low-frequency band (ν_2) corresponds to stretching vibrations of $\text{Fe}^{3+}\text{--O}^{2+}\text{--Fe}^{3+}$ at the B site [15,16].

Table 2. FTIR vibrational mode positions of $\text{Co}_{0.8-x}\text{Mn}_x\text{Zn}_{0.2}\text{Fe}_2\text{O}_4$ Nano ferrite samples.

| x | 0.0 | 0.1 | 0.2 | 0.3 |
|------------------------------|-----|-----|-----|-----|
| ν_1 (cm^{-1}) | 623 | 609 | 585 | 599 |
| ν_2 (cm^{-1}) | 342 | 349 | 409 | 430 |

As presented in **Table 2**, with the increase in the substitution of Mn^{2+} ions, band (ν_1) decreases, whereas band (ν_2) increases. Thus, Mn ions have a greater effect on A sites than B sites. Based on FTIR analysis, the assumed cation distribution of the prepared samples presented in **Table 2** was assumed with the general formula $[\text{Zn}_{0.2}\text{Mn}_{0.8x}\text{Fe}_{0.8-0.8x}]^{\text{A}}[\text{Co}_{0.8-x}\text{Mn}_{0.2x}\text{Fe}_{1.2+0.8x}]^{\text{B}}\text{O}_4$.

Conclusion

The structural and morphological properties of $\text{Co}_{0.8-x}\text{Mn}_x\text{Zn}_{0.2}\text{Fe}_2\text{O}_4$ ($x = 0.0, 0.1, 0.2,$ and 0.3) spinel ferrites were successfully investigated by the coprecipitation method. The prepared samples confirmed the single-phase cubic spinel structure from the XRD patterns. An increase in lattice parameter was observed in the range of $8.3256\text{--}8.377\text{ \AA}$. The average grain size decreases at $x > 0.2$ and subsequently increases at $x = 0.3$. A spherical shape of $\text{Co}_{0.6}\text{Mn}_{0.2}\text{Zn}_{0.2}\text{Fe}_2\text{O}_4$ was concluded from TEM image with an average particle size of 22.51 nm . Two peaks at ~ 442.09 and 620.21 cm^{-1} appeared in the range of $200\text{--}1000\text{ cm}^{-1}$, confirming the formation of the ferrite composite from FTIR analysis shown. The cation distribution of the prepared samples was also predicted to be $[\text{Zn}_{0.2}\text{Mn}_{0.8x}\text{Fe}_{0.8-0.8x}][\text{Co}_{0.8-x}\text{Mn}_{0.2x}\text{Fe}_{1.2+0.8x}]$ ($x = 0.0, 0.1, 0.2,$ and 0.3) from FTIR analysis. The different changes in the structural and morphological properties of Mn-substituted Co–Zn ferrite can be attributed to the rearrangement of cations at different sites.

References

1. Nigam A, Pawar SJ. Structural, magnetic, and antimicrobial properties of zinc doped magnesium ferrite for drug delivery applications. *Ceramics International*. 2020; 46(4):4058-64.

2. Gonçalves JM, de Faria LV, Nascimento AB, Germscheidt RL, Patra S, Hernández-Saravia LP, et al. Sensing performances of spinel ferrites MFe_2O_4 ($M = Mg, Ni, Co, Mn, Cu$ and Zn) based electrochemical sensors: A review. *Analytica Chimica Acta*. 2020 Nov 15;1233:340362.
3. Alghamdi N, Stroud J, Przybylski M, Żukrowski J, Hernandez AC, Brown JM, et al. Structural, magnetic and toxicity studies of ferrite particles employed as contrast agents for magnetic resonance imaging thermometry. *Journal of Magnetism and Magnetic Materials*. 2020;497:165981 .
4. Hankiewicz JH, Stoll JA, Stroud J, Davidson J, Livesey KL, Tvrđy K, et al. Nano-sized ferrite particles for magnetic resonance imaging thermometry. *Journal of Magnetism and Magnetic Materials*. 2019;469:550-7.
5. Li W, Wang W, Lv J, Ying Y, Yu J, Zheng J, et al. Structure and magnetic properties of iron-based soft magnetic composite with Ni-Cu-Zn ferrite-silicone insulation coating. *Journal of Magnetism and Magnetic Materials*. 2018; 456:333-40.
6. Vedrtnam A, Kalauni K, Dubey S, Kumar A. A comprehensive study on structure, properties, synthesis and characterization of ferrites. *AIMS Materials Science*. 2020;7(6):800-35.
7. Ahmad SI. Nano cobalt ferrites: Doping, Structural, Low-temperature, and room temperature magnetic and dielectric properties – A comprehensive review. *Journal of Magnetism and Magnetic Materials*. 2022;562:169840.
8. Ibrahim MA. M.Sc. thesis, "Synthesis and characterization of copper ferrite from copper slimes by wet-chemical methods", Faculty of Science, Al-Azhar University, Cairo, 2009.
9. Sandeep A, Ganesh G, Swathi S, Rajesh N, Sreelatha M. Synthesis, structural, magnetic and optical studies of Eu doped Ni-Zn nano ferrites. *Ceramics International*. 2022;48:29493-501.
10. Rady KE, El Salam ARA, ELFadaly EA, Aly MH. Role of Mn^{2+} ion in the optimization of the structural and dielectric properties of Co-Zn ferrite. *Applied Physics A*. 2023;129:245.
11. Rajasekhar Babu K, Purnachandra Rao M, Subba Rao PSV, Rama Rao K. Influence of Cu Substitution on Physical Properties of Co-Zn Ferrite Nanoparticles. *International Journal of Engineering Research & Technology*. 2017 Jan;6(1).
12. Anu K, Hemalatha J. Magnetic and electrical conductivity studies of zinc doped cobalt ferrite nanofluids. *Journal of Molecular Liquids*. 2019;284:445-453.
13. Das M, Khan MNI, Matin MA, Uddin MM. Structural, Morphological, Electrical and Magnetic Properties of Yttrium-Substituted Co-Zn Ferrites Synthesized by Double Sintering Technique. *Journal of Superconductivity and Novel Magnetism*. 2019;32:3659-77.
14. Jagadeesha Angadi V, Lakshmi prasanna HR, Manjunatha K. Investigation of Structural, Microstructural, Dielectric and Magnetic Properties of Bi^{3+} Doped Manganese Spinel Ferrite Nanoparticles for Photonic Applications. In: Luo Y, Wen J, Zhang J, editors. *Bismuth - Fundamentals and Optoelectronic Applications*. IntechOpen; 2020. 10.5772/intechopen.92430.
15. Jabbar R, Sabeeh SH, Hameed AM. Structural, dielectric and magnetic properties of Mn^{2+} doped cobalt ferrite. *Journal of Magnetism and Magnetic Materials*. 2020;494:165726.
16. Tapdiya S, Shrivastava AK, Singh S. Effect of Mn substitution on structural and magnetic properties of cobalt ferrite. *Advanced Materials Proceedings*. 2017;2(9):547-51.
17. Sharifi I, Shokrollahi H. Magnetic and Mossbauer evaluation of Mn substituted Co-Zn ferrite nanoparticles synthesized by co-precipitation. *Journal of Magnetism and Magnetic Materials*. 2013;334:36-40.
18. Slatineanu T, Iordan AR, Oanca V, Palamaru MN, Dumitru I, Constantin CP, et al. Magnetic and dielectric properties of Co-Zn ferrite. *Materials Science and Engineering*. 2013;178:1040-7.